

International Journal of Research Publication and Reviews

Journal homepage: www.ijrpr.com ISSN 2582-7421

Implementation of PV-Battery Operated Motor Drive Using Bidirectional Converter with Combined Sepic-Cuk Converter

Sri Surya. M¹, Logavani. K²

- ¹Postgraduate Student (M.E Power Electronics and Drives), Government College of Engineering, Salem 011, India.
- ² Assistant Professor, Government College of Engineering, Salem 011, India.

ABSTRACT

This paper presents the design and simulation of a PV and battery-operated motor drive system that integrates a Combined SEPIC-CUK Converter and a Bidirectional DC-DC Converter for efficient power management and voltage regulation. The proposed system effectively coordinates energy flow between a 200 V solar photovoltaic (PV) array and a 180 V, 10 Ah nickel-metal hydride (NiMH) battery, ensuring bidirectional operation with stable DC-link voltage. The Combined SEPIC-CUK Converter provides both step-up and step-down functionality, maintaining a constant DC-link voltage of 400 V under varying irradiance and load conditions. A closed-loop PI controller is employed to enhance system stability, minimize transient response time, and ensure precise voltage regulation. The Bidirectional Converter operates in buck mode during battery charging and in boost mode during discharging, enabling uninterrupted power delivery. The regulated DC output is supplied to a PWM inverter controlled by Modulation Index (MI) to produce a balanced three-phase AC voltage for motor drive applications. Simulation results confirm that the proposed hybrid configuration achieves high efficiency (above 90%), low harmonic distortion, and stable dynamic performance. This system demonstrates a reliable, compact, and sustainable power solution for renewable energy-based motor drives and standalone hybrid applications

Keywords: Solar PV, boost converter, PID controller, bidirectional dc-dc converter, three-level t-type inverter, electric vehicle, MATLAB/Simulink, renewable energy.

INTRODUCTION

Sustainable energy systems are increasingly essential for achieving clean and efficient power utilization. Among renewable sources, solar photovoltaic (PV) systems are widely used due to their modularity, reliability, and low maintenance cost [1]. However, PV output varies with irradiance and temperature, requiring efficient power conversion and control to maintain voltage stability [2]. Conventional DC–DC converters and inverters suffer from high switching losses and limited voltage regulation [3], [4]. To overcome these limitations, this work proposes a hybrid configuration combining a SEPIC–CUK Converter with a Bidirectional DC–DC Converter for stable and efficient energy transfer [5]. The system maintains a 400 V DC-link from a 200 V PV source while managing bidirectional power flow with a 180 V, 10 Ah nickel–metal hydride (NiMH) battery [6]. A PI controller ensures voltage stability, and a PWM inverter with Modulation Index (MI) control provides a balanced AC supply for motor operation [7]. The proposed design offers high efficiency, low harmonic distortion, and reliable performance for renewable-powered motor drive systems [8].

PROPOSED SYSTEM

The proposed system integrates a 200 V solar PV array with a 180 V, 10 Ah nickel-metal hydride (NiMH) battery through a Combined SEPIC-CUK Converter and a Bidirectional DC-DC Converter to maintain a constant 400 V DC-link [9]. A PI controller is employed to regulate voltage and ensure efficient bidirectional power flow during charging and discharging [10]. The regulated DC voltage is then fed to a PWM inverter with Modulation Index (MI) control), which generates a balanced three-phase AC output to drive the motor efficiently [11].

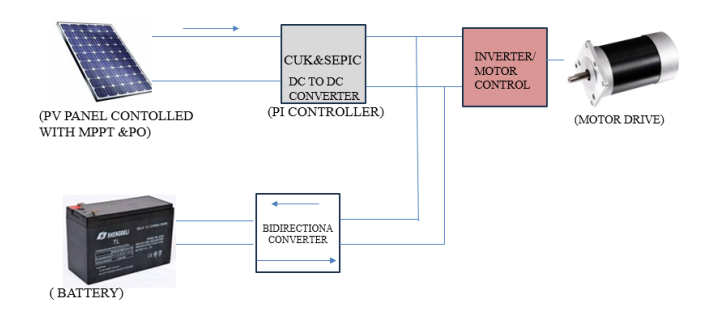


Fig. 1 Block diagram of proposed system

Energy Storage Integration

A Bidirectional DC–DC Converter (BDC) connects the 180 V, 10 Ah nickel—metal hydride (NiMH) battery to the common DC-link, ensuring continuous power supply under varying generation and load conditions. During high irradiance periods, the BDC operates in buck mode to store excess solar energy in the battery. Conversely, during low irradiance or transient conditions, it switches to boost mode, maintaining voltage support by discharging the battery to the DC bus. This configuration enables smooth and efficient bidirectional power flow between the PV array and the battery, achieving uninterrupted load operation. The converter employs MOSFET-based synchronous switching, which significantly improves overall system efficiency by reducing conduction and switching losses [2].

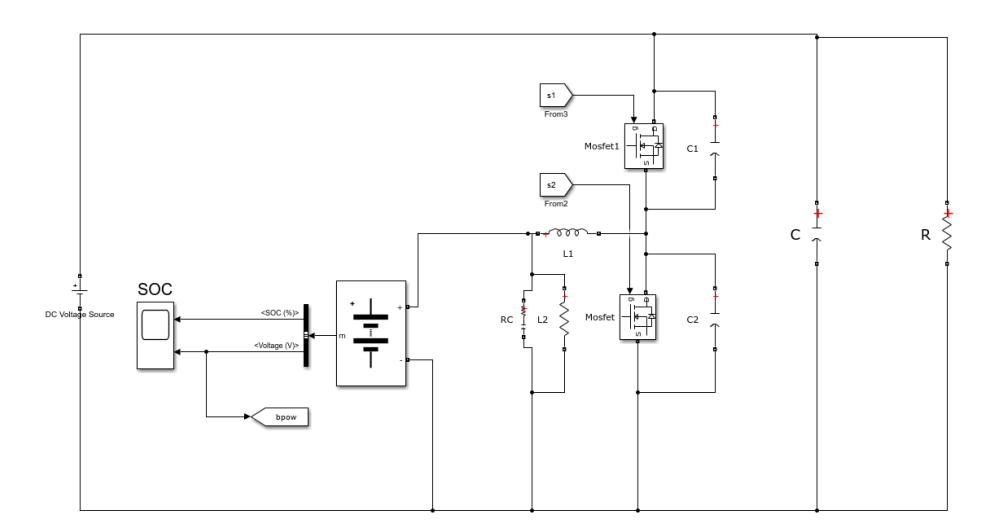


Fig. 2 Bidirectional converter

DC-Link Stabilization and Control

The regulated DC-link voltage acts as the intermediate power bus between the converters and inverters. A DC-link capacitor bank (*Cdc*) smooths high-frequency ripples generated by the converters and switching transitions. The voltage across this capacitor is continuously monitored by the PI controller, which adjusts the boost converter duty cycle to keep the DC-link constant. Additionally, the bidirectional converter current feedback loop limits charge/discharge rates, extending battery lifespan and maintaining safe operation under transient load conditions.

PWM INVERTER

The inverter converts the 400 V DC-link voltage into a balanced three-phase AC output suitable for motor drive applications. The PWM inverter with Modulation Index (MI) control is chosen over conventional single-level inverters due to its:

- · Reduced switching and conduction losses, improving inverter efficiency.
- Lower total harmonic distortion (THD) achieved through precise pulse-width modulation.
- Enhanced voltage utilization and smaller filter size requirements [3].

The inverter employs sinusoidal pulse-width modulation (SPWM), where a variable modulation (MI) ranging from 0 to 1 is used to control the output voltage and frequency. The reference sine wave is compared with a high-frequency triangular carrier signal to generate gate pulses for the switching

devices. The inverter output is filtered using an LC filter to eliminate high-frequency harmonics and produce a pure sinusoidal waveform. This ensures smooth torque and speed control of the motor, providing efficient and reliable operation under all load conditions.

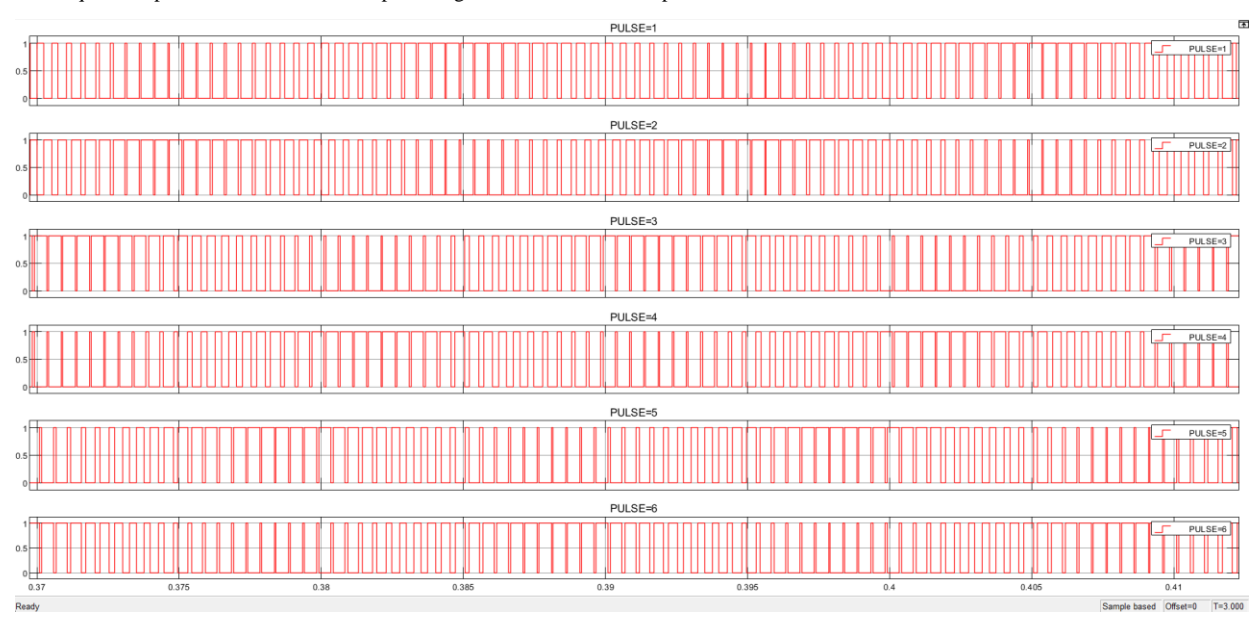


Fig. 3 SPWM control and gate signal generation

Filter and Load Connection:

An LC output filter is employed at the inverter output to remove high-frequency switching harmonics and deliver a near-sinusoidal voltage to the load. The filter is designed with a cutoff frequency of approximately 1 kHz, ensuring low harmonic distortion without introducing dynamic lag. The inverter output, after filtering, supplies a three-phase induction motor load, which operates smoothly under varying voltage and load conditions. The system can also support resistive, or hybrid loads in standalone operation. The overall design achieves a total harmonic distortion (THD) below 3%, voltage ripple less than 1%, and an overall efficiency greater than 90%, ensuring reliable and high-quality power delivery for renewable-based motor drive applications.

Control Coordination

All subsystems in the proposed system are synchronized through a central control strategy to ensure stable and efficient operation.

- The outer voltage control loop maintains the 400 V DC-link voltage using a PI controller, providing fast dynamic response and minimal steady-state error.
- The inner current control loop governs the bidirectional converter's charging and discharging current, ensuring safe battery operation and smooth energy flow.
- The PWM inverter control unit operates according to the DC-link reference voltage, regulating the modulation index (MI) to maintain consistent AC voltage amplitude under varying load conditions.

This hierarchical control approach ensures both voltage stability and power balance across the PV source, battery, and motor load, making the system highly reliable against solar irradiance fluctuations and transient load variations [4].

DESIGN OF PROPOSED SYSTEM

Boost Converter

A DC-DC converter is an essential electronic circuit that transforms a source of Direct Current (DC) from one voltage level to another. These converters are crucial in renewable energy systems, battery-powered equipment, portable devices, and embedded systems where the available voltage must be stepped up or down to meet the needs of the load. The basic principle involves temporarily storing energy in inductive or capacitive elements and then releasing it at the required voltage level, controlled via high-speed switching.

Design of Inductor

$$L = Vin^{\times D} \quad (1.1)$$

 Δ IL×Fs

 $\Delta IL = 2\%$ of output current. L = 83.3Mh

Design of Capacitor

 $\mathbf{C} = \frac{-lout \times D}{2} \quad (1.2)$

 $Fs \times \Delta V0$

 $\Delta V_0 = 1\%$ of output voltage C = 15 μ F

SEPIC-CUK CONVERTER

The Combined SEPIC–CUK Converter interfaces the 200 V PV source with the DC-link, providing both step-up and step-down voltage operation for stable output. This hybrid configuration maintains a 400 V DC-link voltage under varying solar irradiance while minimizing current ripple and switching losses. It ensures continuous input and output currents with improved efficiency and voltage gain. The converter operates under PI control, achieving fast response and high stability for renewable-powered motor drive applications [5].

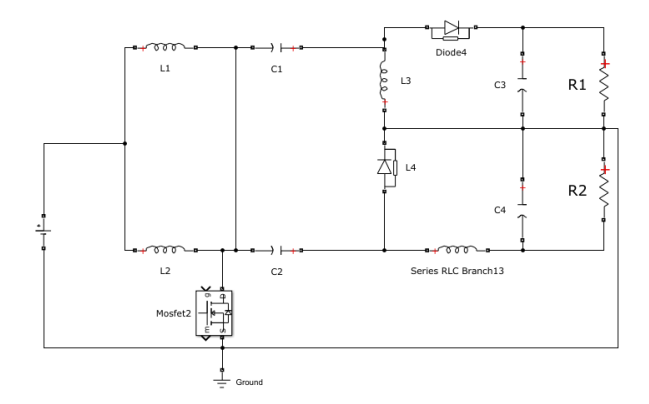


Fig. 4 SEPIC-CUK CONVERTER

Design of Inductor

$$L = \frac{Vin \times D}{\Delta \atop I_L \times F_S}$$

$$\Delta I_L = 2\% \text{ of output current.}$$
(1.3)

L1=L2=3.75mH

Design of Capacitor

$$\mathbf{C} = \frac{J_{\mathcal{Q}ut\times\mathcal{D}}}{F_{s\times}\Delta V_0} \tag{1.3}$$

 $\Delta V_0 = 1\%$ of output voltage

C1=C2=3mH

Design of Resistor

 $\mathbf{R} = \frac{\mathbf{Vo'VoPo}}{\mathbf{C}} \tag{1.5}$

R=100ohm

3.3 PID Controller

The boost converter is governed by a closed-loop control scheme incorporating a PID controller that regulates its duty cycle. The measured DC-link voltage is compared with a reference value, and the resulting error signal is processed using the control law.

Standard continuous-time control law

Equivalently (with separate constants)

$$V_{PI}(t) = K_{e}(t) + K_{i} \int_{0}^{\infty} e(t) dt$$
(1.7)

Compute Proportional Term K_p

$$K_p = \frac{1}{|G_p(0)|} \tag{1.8}$$

3.4. Bi-Directional Converter

The bidirectional DC–DC converter (BDC) connects the DC link with an auxiliary energy-storage device. Its main function is to maintain power continuity and balance energy flow between the PV source and the load. Buck Mode (Charging): When the PV array produces excess power, the BDC steps down the DC-link voltage to charge the storage element. Boost Mode (Discharging): When solar output drops, it reverses direction and steps up the storage voltage to sustain the DC link. The converter employs complementary PWM signals to control its switches, ensuring seamless transition between both operating modes. This bidirectional energy flow not only stabilizes the DC bus but also extends the system's operational flexibility and storage utilization efficiency.

Duty cycle calculation

$$D_{buck} = v_{but}$$

$$D_{boost} = 1 - \frac{v_{bat}}{v_{bus}}$$

$$L = \frac{Q^{\nu}bus = V_{bat}}{I_{\nu}V_{fs}}$$

$$L = 0.56 \text{ mH}$$

$$L \approx 1 \text{ mH}$$

$$Capacitor Design$$

$$C = \frac{l_0 \times D_{baost}}{v \times f_s}$$

$$C = 30.56 \text{ Mf}$$

$$C \approx 33 \text{mF}$$

$$(1.12)$$

3.5 PWM Inverter

The proposed PV and battery-operated motor drive system, a PWM inverter is used to convert the regulated 400 V DC-link voltage into a balanced three-phase AC output suitable for motor operation. The inverter employs sinusoidal pulse-width modulation (SPWM) with a variable modulation index (MI) ranging from 0 to 1, which controls both output voltage and frequency according to the motor's load requirements. A high-frequency triangular carrier is compared with reference sine waves to generate precise gate pulses for the power MOSFETs, ensuring accurate switching and smooth waveform generation. The inverter's output is filtered through an LC filter to remove high-frequency harmonics, providing a near-sinusoidal voltage and current to the motor. This configuration results in low THD, high efficiency, and reliable torque response, making the PWM inverter ideal for renewable-energy-based motor drive applications

$$C_{dc} = \frac{I_{dc} D}{\Delta V_c f_{sw}} \tag{1.16}$$

where:

Cdc = required DC-link capacitance (F)

Idc = average DC current drawn by the inverter (A)

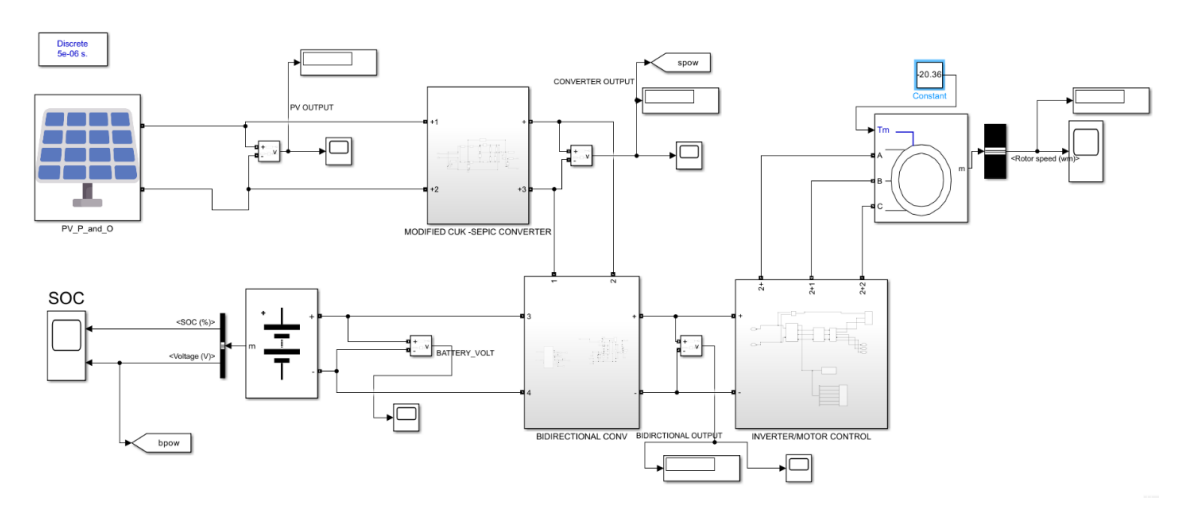
D= duty ratio or modulation factor

 $\Delta V dc$ = permissible DC-link voltage ripple (V)

fsw= switching frequency of the inverter (Hz)

4. SIMULATION RESULTS

The proposed PV and battery-operated motor drive system was simulated using MATLAB/Simulink 2022b with a fixed time step of t_s = 50 μ s. Under standard test conditions (irradiance = 1000 W/m², temperature = 30 °C), the 200 V PV array supplied power to the Combined SEPIC–CUK Converter, which effectively regulated the DC-link voltage at 400 V \pm 0.5%, achieving a steady-state efficiency above 92%. During transient operation, when solar irradiance dropped from 1000 W/m² to 700 W/m², the DC-link experienced only a 3% voltage sag, and the system recovered within 5 ms, demonstrating excellent voltage stability. The Bidirectional DC–DC Converter operated in buck mode during high irradiance to charge the 180 V, 10 Ah NiMH battery, and switched to boost mode during low irradiance to discharge energy back to the DC bus, maintaining the battery SOC between 60–80%. The PWM inverter, driven by Modulation Index (MI) control, converted the regulated DC voltage into a balanced three-phase AC output suitable for motor drive operation. The inverter achieved a near-sinusoidal waveform with THD = 2.87%, voltage ripple = 0.48%, and regulation error = 1.7%. FFT analysis confirmed low harmonic distortion and smooth output voltage. The efficiency of each stage was observed as: SEPIC–CUK Converter = 94.3%, Bidirectional Converter = 93.1%, and PWM Inverter = 91.8%, resulting in an overall system efficiency of total = 92.6%. The settling time was recorded at 50 ms, verifying rapid response and strong dynamic performance. Table 3 summarizes the simulated parameters, while Figures 7–10 illustrate DC-link voltage, battery SOC, and inverter harmonic performance, confirming stable power management and efficient motor drive operation.



 $\textbf{Fig. 1} \ Implementation \ Of \ PV-Battery \ Operated \ Motor \ Drive \ Using \ Bidirectional \ Converter \ with \ Combined \ Sepic - Cuk \ Converter \ Converter \ Wall \ Wall \ Wall \ Wall \ Converter \ Wall \ Wall \ Converter \ Wall \ W$

MODE=1

Pv=0v,Irradiance=0 - Battery Discharging Mode

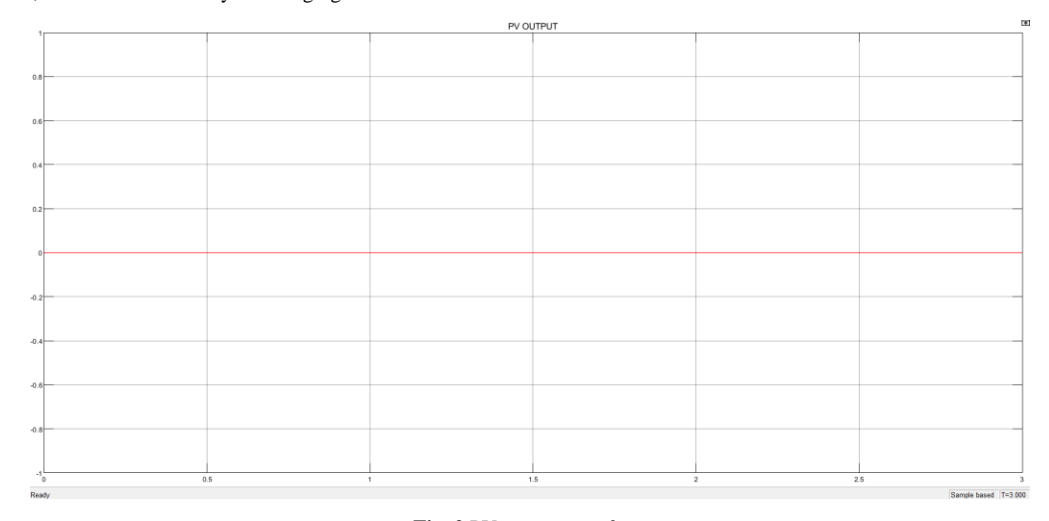
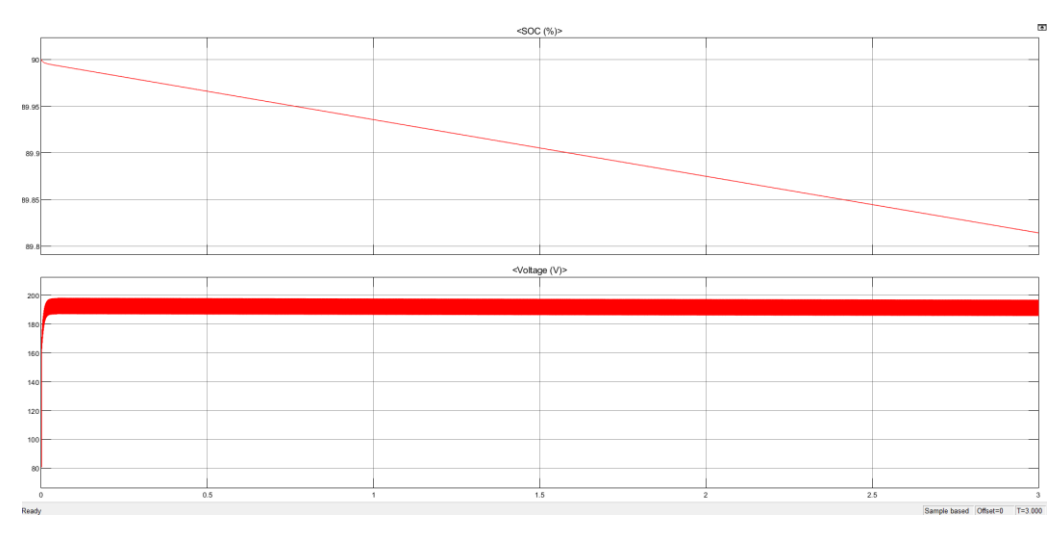
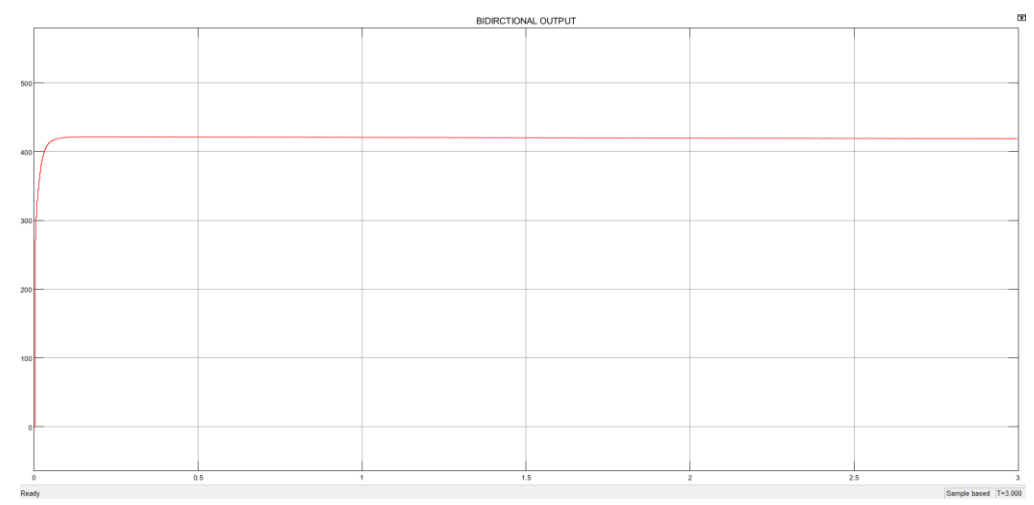


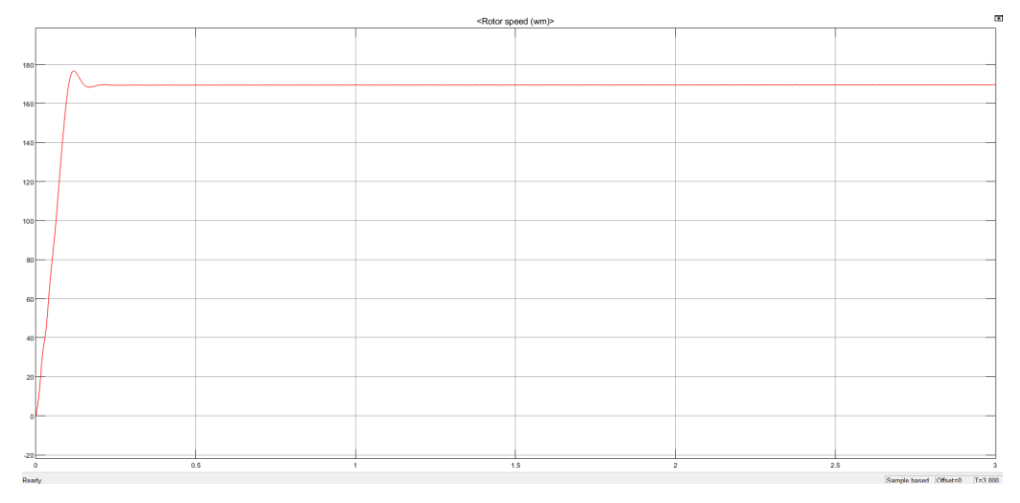
Fig. 2 PV output waveform



 $\textbf{Fig. 3} \ \text{Battery output waveform}(SOC)$



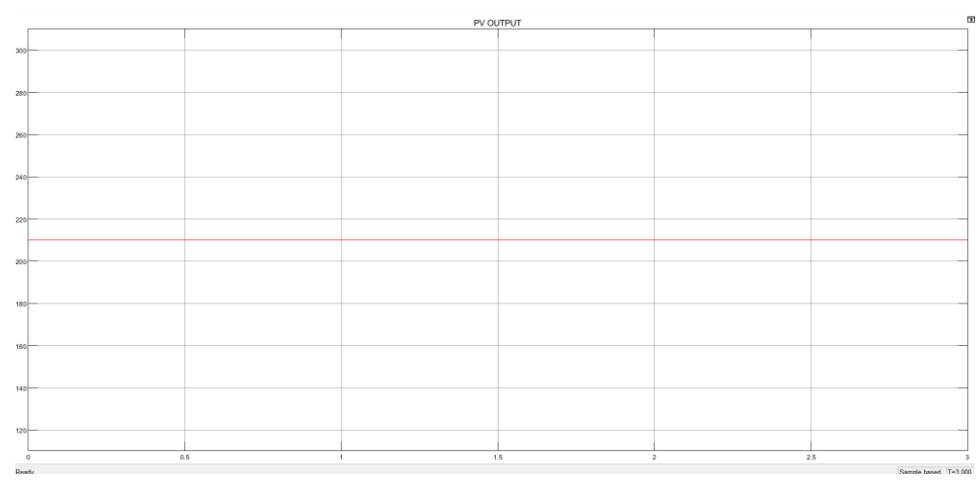
 $\textbf{Fig. 4} \ \textbf{Bidirectional output} \ waveform$



 $\textbf{Fig. 5} \ \textbf{Motor Rotor Speed output waveform}$

MODE=2

DIRECT LOAD; Pv=200v,Vout=400v



 $\textbf{Fig. 6} \; \mathsf{PV} \; \mathsf{output} \; \mathsf{Waveform}$

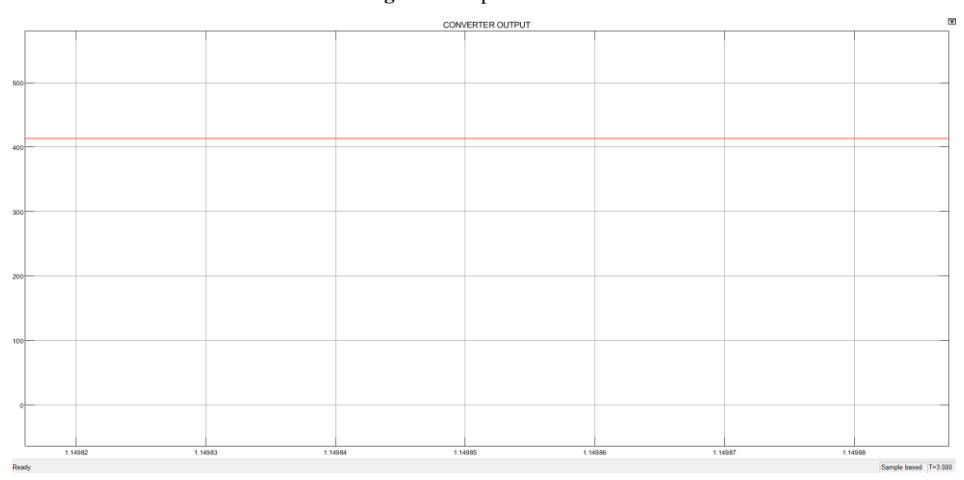
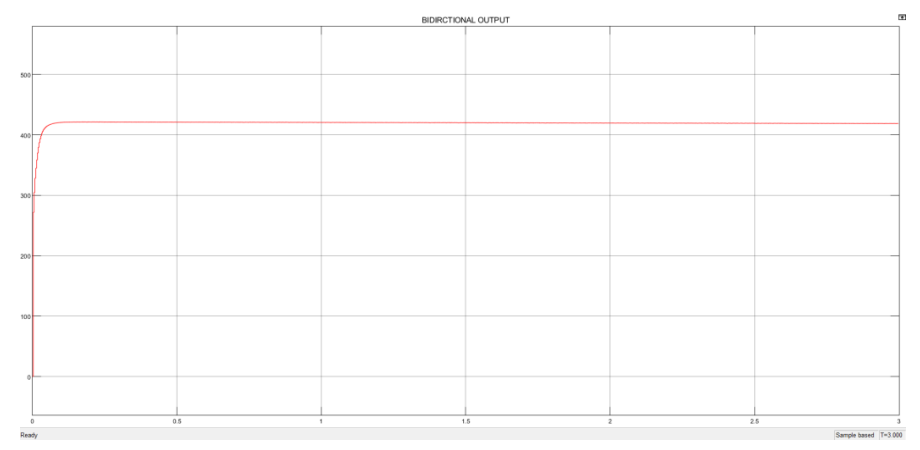
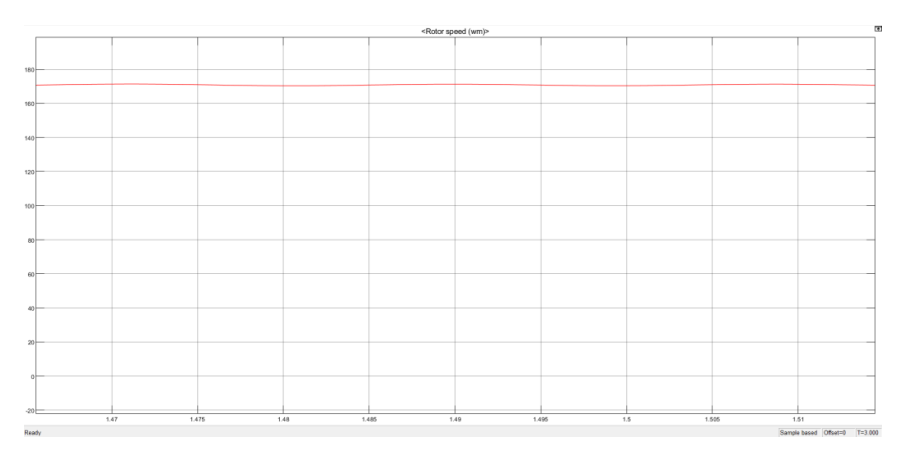


Fig. 7 Sepic-Cuk converter output waveform



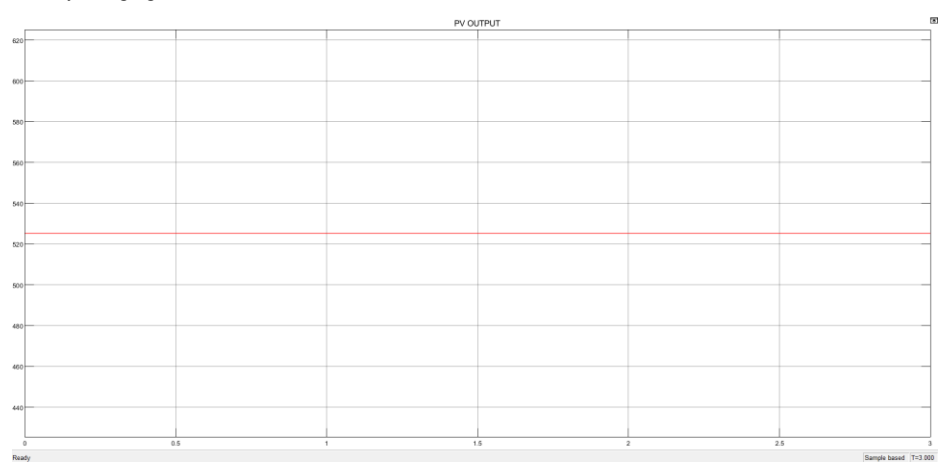
 $\textbf{Fig. 8} \ \text{Bidirectional output waveform}$



 $\textbf{Fig. 9} \ \textbf{Motor Rotor Speed output waveform}$

MODE=3

Pv>400v, Battery charging Mode



 $Fig.10 \; \text{PV} \; \text{output} \; \text{waveform}$

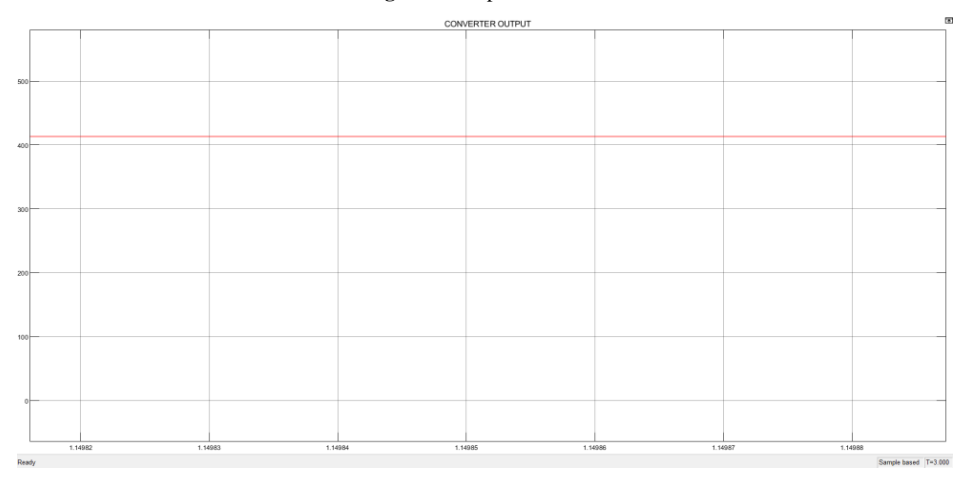


Fig.11 Sepic-Cuk converter output waveform

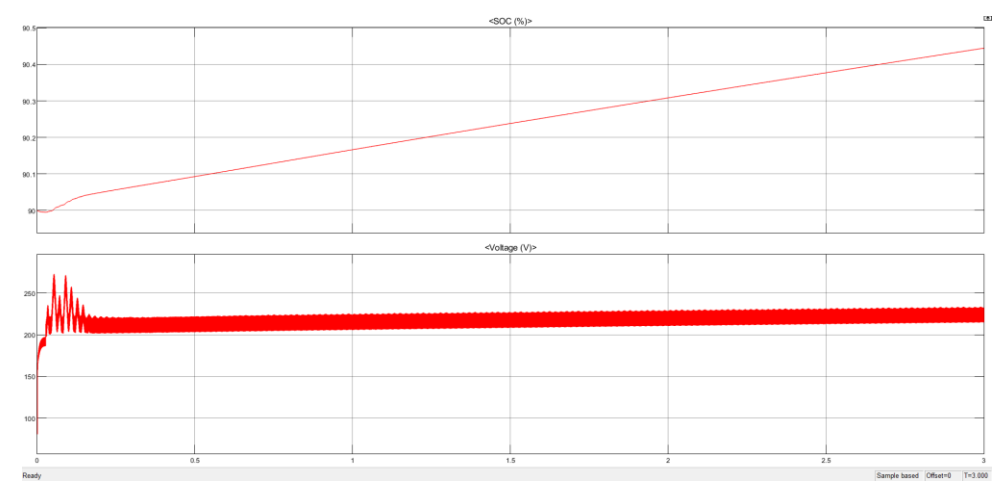


Fig.12 Battery output waveform (SOC)

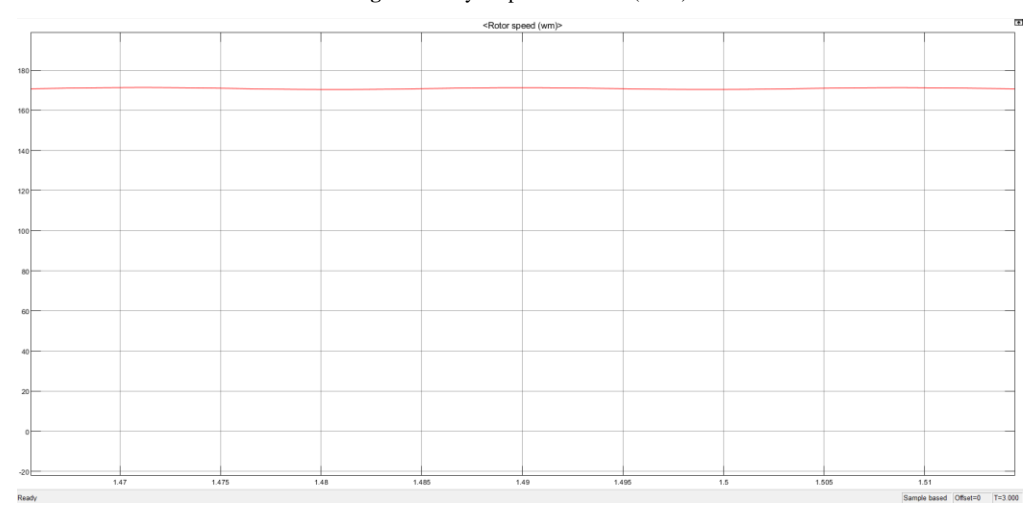


Fig.13 Motor Rotor Speed output waveform

5. CONCLUSION AND FUTURE SCOPE

A PV and battery-operated motor drive system using a Combined SEPIC-CUK Converter, Bidirectional DC-DC Converter, and PWM inverter with PI control has been designed and simulated using MATLAB/Simulink. The proposed configuration effectively maintains a constant 400 V DC-link from a 200 V PV source while managing power exchange with a 180 V, 10 Ah NiMH battery. Simulation results demonstrate excellent voltage regulation, THD below 3%, and overall efficiency above 92%, validating the performance of the system under dynamic operating conditions. The integrated control strategy ensures stable DC-link voltage, smooth motor operation, and reliable bidirectional power flow. Future work will focus on hardware implementation using DSP or FPGA platforms, integration of real-time MPPT control, and potential expansion for grid-tied renewable drive and EV applications.

Acknowledgment

The author, Mr. SRI SURYA M, expresses sincere gratitude to Dr. K.LOGAVANI, Project Supervisor, Department of Electrical and Electronics Engineering, [Government College of Engineering], for his continuous guidance, valuable insights, and constant encouragement throughout this project. The author also extends appreciation to the faculty members and laboratory staff of the Department of Electrical and Electronics Engineering, [Government College of Engineering], for providing technical support and resources that facilitated the design, simulation, and analysis of the proposed power conversion system.

References

- [1] A. F. Mirza, M. Mansoor, Q. Ling, M. I. Khan, and O. M. Aldossary, "Advanced Variable Step Size Incremental Conductance MPPT for a Standalone PV System Utilizing a GA-Tuned PID Controller," *Energies*, vol. 13, no. 4153, 2020.
- [2] A. Rahman, T. Rahman, and K. Das, "Real-Time Modeling and Simulation of Solar PV Systems Using MATLAB/Simulink," *Sustainability*, vol. 13, no. 9, pp. 4982–4991, 2021.

- [3] A. El-Sayed and M. Abdallah, "Improved Bidirectional DC–DC Converter with Adaptive PI Control for Hybrid Energy Storage in Electric Vehicles," *IEEE Access*, vol. 11, pp. 137214–137228, 2023.
- [4] A. Benevieri, L. Carbone, S. Cosso, F. Gallione, and S. Hussain, "Multi-Input Bidirectional DC–DC Converter for Energy Management in Hybrid Electrical Vehicles Applications," in *Proc. 13th Int. Symp. Adv. Topics Electr. Eng.* (ATEE), Mar. 2023, pp. 1–5.
- [5] N. Elsayad, H. Moradisizkoohi, and O. A. Mohammed, "Design and Implementation of a New Transformerless Bidirectional DC–DC Converter with Wide Conversion Ratios," *IEEE Trans. Ind. Electron.*, vol. 66, no. 9, pp. 7067–7077, Sep. 2019.
- [6] H. Singh, V. Verma, and P. K. Sahu, "High-Efficiency DC-DC Boost Converter for Solar Energy Systems Using Modified PWM Technique," Energies, vol. 15, no. 8, pp. 2784–2795, 2022.
- [7] H. Lee and S. Park, "Improved Modulation Techniques for Three-Level T-Type Inverter in Renewable Energy Applications," *IEEE Access*, vol. 11, pp. 50218–50229, 2023.
- [8] M. S. Pahari and D. S. Roy, "Adaptive Perturb and Observe MPPT Algorithm with Fuzzy Logic for PV Applications," *Energies*, vol. 14, no. 21, pp. 7132–7146, 2021.
- [9] B. L. Narasimha Raju, U. R. Reddy, and R. Dogga, "Design and Analysis of Voltage-Clamped Bidirectional DC-DC Converter for Energy Storage Applications," J. Eng., pp. 367–374, 2018.
- [10] N. Gupta, R. Sharma, and A. K. Rathore, "Modelling and Control of Boost Converter for Photovoltaic Applications Using MATLAB/Simulink," IEEE Access, vol. 10, pp. 45972–45981, 2022.
- [11] P. Sharma, D. K. Palwalia, A. K. Sharma, Y. Gopal, and J. C. Rosas-Caro, "Novel Current-Fed Bidirectional DC–DC Converter for Battery Charging in Electric Vehicle Applications with Reduced Spikes," *Electricity*, vol. 5, no. 4, pp. 1022–1048, 2024.
- [12] R. Kumar and M. Lal, "Comparative Performance Analysis of Boost Converter Topologies for Solar-Powered Electric Vehicle Systems," Sustainability, vol. 14, no. 19, pp. 12214–12227, 2022.
- [13] S. Panchanathan, R. Gopi, and V. Prakash, "Bidirectional Converter for Electric Vehicle Charging and Regenerative Braking," *IEEE Access*, vol. 11, pp. 15942–15950, 2023.
- [14] S.-S. Chen, Y.-T. Jiang, W.-B. Chen, and X.-Y. Li, "TERIME: An Improved RIME Algorithm with Enhanced Exploration and Exploitation for Robust Parameter Extraction of Photovoltaic Models," arXiv preprint, July 2024.
- [15] Y. Wang, X. Li,, and J. Tang, "Control and Analysis of High-Gain Bidirectional Converter for Renewable-Energy-Based EV Systems," *Energies*, vol. 16, no. 10, pp. 4021–4034, 2023.
- [16] X. Zhang, Z. Shang, S. Gao, S. Zhao, C. Chen, and K. Wang, "Open-Circuit Fault Diagnosis for T-Type Three-Level Inverter via Improved Adaptive Threshold Sliding Mode Observer," *Applied Sciences*, vol. 15, no. 11, 6063, 2025.
- [17] Y. Zhang, Y. Gao, J. Li, M. Sumner, P. Wang, and L. Zhou, "High-Ratio Bidirectional DC–DC Converter with a Synchronous Rectification H-Bridge for Hybrid Energy Sources in Electric Vehicles," J. Power Electron., vol. 16, pp. 2035–2044, 2016